

Metadata of the article that will be visualized in OnlineFirst

ArticleTitle	Long-read sequencing reveals increased isoform diversity in key transcription factor effectors of intercellular signalling at the invertebrate-vertebrate transition	
<hr/>		
Article Sub-Title		
Article CopyRight	The Author(s) (This will be the copyright line in the final PDF)	
Journal Name	BMC Biology	
Corresponding Author	FamilyName Particle Given Name Suffix Division Organization Address Phone Fax Email URL ORCID	Ferrier David E. K. The Scottish Oceans Institute, School of Biology University of St Andrews St Andrews, Fife, KY16 8LB, UK dekf@st-andrews.ac.uk
Author	FamilyName Particle Given Name Suffix Division Organization Address Division Organization Address Phone Fax Email URL ORCID	Torres-Aguila Nuria P. The Scottish Oceans Institute, School of Biology University of St Andrews St Andrews, Fife, KY16 8LB, UK Current address: Departament de Genètica, Microbiologia I Estadística, Facultat de Biologia, Institut de Recerca de La Biodiversitat (IRBio) Universitat de Barcelona Barcelona, 08028, Spain
Author	FamilyName Particle Given Name Suffix Division Organization Address Division Organization Address Phone Fax Email URL Email	Salonna Marika Institute of Medical Sciences Foresterhill Health Campus, University of Aberdeen Aberdeen, AB25 2ZD, UK Current address: School of Molecular Biosciences, College of Medical, Veterinary & Life Sciences University of Glasgow Glasgow, G12 8QQ, UK

	URL	
	ORCID	
Author	FamilyName Particle Given Name Suffix Division Organization Address Phone Fax Email URL ORCID	Shimeld Sebastian M. The Department of Biology University of Oxford, Life and Mind Building South Parks Road, Oxford, OX1 3EL, UK
Author	FamilyName Particle Given Name Suffix Division Organization Address Phone Fax Email URL ORCID	Hoppler Stefan Institute of Medical Sciences Foresterhill Health Campus, University of Aberdeen Aberdeen, AB25 2ZD, UK
Schedule	Received Revised Accepted	23 May 2025 16 Jan 2026
Abstract	<p><i>Background:</i> Several intercellular signalling pathways (including wingless (Wnt), hedgehog (Hh), and bone morphogenetic protein (BMP)) are used repeatedly in animals throughout development and evolution and are also frequent targets for disease-associated disruptions. We have previously shown that the major transcriptional effectors of β-catenin-dependent Wnt signalling, the TCF/LEF proteins, in contrast to other pathway components, have a higher gene number and isoform diversity in vertebrates versus invertebrates, but this increased diversity has only been poorly quantified. Considering that isoform diversity correlates with organism complexity, any increase in major signalling effectors is likely to have made a significant contribution to vertebrate evolution.</p> <p><i>Results:</i> Using de novo long-read transcriptomes, we compared isoform number per gene for the chordates <i>Ciona intestinalis</i>, <i>Lampetra planeri</i> and <i>Xenopus tropicalis</i>, thus encompassing the invertebrate sister group to vertebrates, as well as a cyclostome and a gnathostome vertebrate. We find a significant increase in the number of transcript isoforms per gene expressed during embryo development and organogenesis at the invertebrate-to-vertebrate transition, specifically for the main transcription factor effectors of the Wnt/β-catenin, Hh and BMP pathways, i.e. TCF/LEF, GLI and SMAD.</p> <p><i>Conclusions:</i> Our results implicate an increase in isoform diversity of the transcription factors of major intercellular signalling pathways as having a disproportionate role in the evolutionary origin and diversification of vertebrates.</p>	
Keywords (separated by '-')	TCF - SMADs - GLIs - <i>Ciona</i> - Lamprey - <i>Lampetra planeri</i> - <i>Xenopus tropicalis</i> - Splicing	
Footnote Information	The online version contains supplementary material available at https://doi.org/10.1186/s12915-026-02522-w .	

1

RESEARCH

Open Access



Long-read sequencing reveals increased isoform diversity in key transcription factor effectors of intercellular signalling at the invertebrate-vertebrate transition

Nuria P. Torres-Aguila^{1,2}, Marika Salonna^{3,4}, Sebastian M. Shimeld⁵, Stefan Hoppler³ and David E. K. Ferrier^{1*}

7

Abstract

AQ1

Background Several intercellular signalling pathways (including wingless (Wnt), hedgehog (Hh), and bone morphogenetic protein (BMP)) are used repeatedly in animals throughout development and evolution and are also frequent targets for disease-associated disruptions. We have previously shown that the major transcriptional effectors of β -catenin-dependent Wnt signalling, the TCF/LEF proteins, in contrast to other pathway components, have a higher gene number and isoform diversity in vertebrates versus invertebrates, but this increased diversity has only been poorly quantified. Considering that isoform diversity correlates with organism complexity, any increase in major signalling effectors is likely to have made a significant contribution to vertebrate evolution.

15

Results Using de novo long-read transcriptomes, we compared isoform number per gene for the chordates *Ciona intestinalis*, *Lampetra planeri* and *Xenopus tropicalis*, thus encompassing the invertebrate sister group to vertebrates, as well as a cyclostome and a gnathostome vertebrate. We find a significant increase in the number of transcript isoforms per gene expressed during embryo development and organogenesis at the invertebrate-to-vertebrate transition, specifically for the main transcription factor effectors of the Wnt/ β -catenin, Hh and BMP pathways, i.e. TCF/LEF, GLI and SMAD.

21

Conclusions Our results implicate an increase in isoform diversity of the transcription factors of major intercellular signalling pathways as having a disproportionate role in the evolutionary origin and diversification of vertebrates.

23

Keywords TCF, SMADs, GLIs, *Ciona*, Lamprey, *Lampetra planeri*, *Xenopus tropicalis*, Splicing

AQ2

*Correspondence:

David E. K. Ferrier
dekf@st-andrews.ac.uk

¹ The Scottish Oceans Institute, School of Biology, University of St Andrews, St Andrews, Fife KY16 8LB, UK

² Current address: Departament de Genètica, Microbiologia i Estadística, Facultat de Biologia, Institut de Recerca de la Biodiversitat (IRBio), Universitat de Barcelona, Barcelona 08028, Spain

³ Institute of Medical Sciences, Foresterhill Health Campus, University of Aberdeen, Aberdeen AB25 2ZZ, UK

⁴ Current address: School of Molecular Biosciences, College of Medical, Veterinary & Life Sciences, University of Glasgow, Glasgow G12 8QQ, UK

⁵ The Department of Biology, University of Oxford, Life and Mind Building, South Parks Road, Oxford OX1 3EL, UK

Background

The driving forces for the evolution of organism complexity has been a topic of discussion for decades [1–4]. Despite genome duplications being renowned for the creation of new paralogous gene copies and their subsequent evolution via processes like sub- and neofunctionalisation [5], and specialisation [6], the G-value paradox showed that the number of genes in a genome do not necessarily correlate with organism complexity [2]. One of the proposed alternatives to solve this paradox is the expansion of the organism proteome through alternative splicing, correlating with phenotypic novelty

24

AQ3

25

26

27

28

29

30

31

32

33

34

35



© The Author(s) 2026. **Open Access** This article is licensed under a Creative Commons Attribution-NonCommercial-NoDerivatives 4.0 International License, which permits any non-commercial use, sharing, distribution and reproduction in any medium or format, as long as you give appropriate credit to the original author(s) and the source, provide a link to the Creative Commons licence, and indicate if you modified the licensed material. You do not have permission under this licence to share adapted material derived from this article or parts of it. The images or other third party material in this article are included in the article's Creative Commons licence, unless indicated otherwise in a credit line to the material. If material is not included in the article's Creative Commons licence and your intended use is not permitted by statutory regulation or exceeds the permitted use, you will need to obtain permission directly from the copyright holder. To view a copy of this licence, visit <http://creativecommons.org/licenses/by-nc-nd/4.0/>.

Journal : BMC Two 12915	Dispatch : 19-1-2026	Pages : 13
Article No : 2522	<input type="checkbox"/> LE	<input type="checkbox"/> TYPESET
MS Code :	<input checked="" type="checkbox"/> CP	<input checked="" type="checkbox"/> DISK

[3]. Previous studies found a strong correlation between number of cell types (as a proxy for organism complexity) and alternative splicing [4, 7], providing evidence of the importance of isoform diversity for organism evolution. However, whether particular types of genes contribute disproportionately to this phenomenon has not been assessed.

Wnt signalling is a cell-to-cell signalling mechanism highly conserved in the animal kingdom and required during development and regeneration [8]. The best described Wnt pathway is the canonical Wnt (cWnt) pathway, also known as the Wnt/β-catenin pathway, which involves the nuclear translocation of β-catenin, triggered by extracellular Wnt ligand-receptor interactions. Nuclear β-catenin functions as a co-regulator for activation of Wnt-target genes, usually via binding the T-cell factor/lymphoid enhancer factor (TCF/LEF) proteins. The cWnt pathway has a variety of roles in animal homeostasis and development, including involvement in development of the anterior-posterior and dorsal-ventral axes [8, 9]. It is also associated with many human diseases such as cancers [10], diabetes [11] and mental disorders [12]. Comparably widespread functions in development, homeostasis and disease are also seen in other major signalling systems such as the hedgehog (Hh) and bone morphogenetic protein (BMP) pathways, whose main transcription factors are the Glioma-Associated Oncogene (GLI) proteins and the small/Mothers Against DPP Homolog (SMAD) proteins, respectively [13–15].

Genome comparisons between vertebrates and invertebrates reveal a remarkable conservation of the cWnt pathway with relatively little expansion of most of its components [16]. Nonetheless, vertebrate TCF/LEF transcription factors, the main transcription factor of the cWnt pathway, show a much greater diversity [17–20]. Multiple copies of TCF/LEF genes have been retained from genome duplications in vertebrates, which typically possess four TCF/LEF family genes with multiple isoforms, while invertebrates typically have one TCF gene with a single isoform [20, 21]. A similar gene expansion might have occurred for SMAD and GLI families of transcription factors mediating BMP/TGFβ and Hh signalling, respectively.

Given these general observations, we aimed to assess transcript isoform diversity of developmentally expressed genes across components of these signalling pathways (cWnt–TCF/LEF, BMP–SMAD, Hh–GLI) and compare them to other categories of genes. We hypothesised that such major developmental control genes may have been a particular target for the evolutionary diversification that occurred with the origin of the vertebrates. We selected three species representing key lineages of the Olfactores

chordates; the invertebrate urochordate *Ciona intestinalis*, the cyclostome (jawless vertebrate) *Lampetra planeri*, and a gnathostome (jawed vertebrate) *Xenopus tropicalis*, to analyse in an unbiased way the number of genes and transcripts expressed during embryogenesis and assess if TCF/LEF, SMAD and GLI genes are distinctive in their transcript isoform diversity. Our use of de novo long-read sequencing data was focused specifically on selected developmental stages of the three chosen species to help overcome the difficulty in accurately and reliably determining splice isoforms from short-read sequencing data. Also, our approach allows us to determine which genes and isoforms are specifically deployed during development to improve the comparability of our data between species.

Results

Transcriptome analysis

To analyse the diversity of isoforms of developmentally transcribed genes within chordates, we performed cDNA long-read sequencing of developmental stages of *C. intestinalis*, *L. planeri* and *X. tropicalis* (see Table 1) and processed the data following the pipeline shown in Fig. 1. All selected stages performed similarly in the sequencing protocol (Table 1) producing de novo transcriptomes with loci coverage over 40% (Fig. 2A) and capturing over 60% of metazoan-conserved orthologues (BUSCOs) (Fig. 2D). Notably, the transcriptomes included over 10% of novel loci, with gene models not currently annotated in the respective reference genomes (Fig. 2B), although the highest proportion of transcripts were ones that fully matched reference models (categories ‘=’, ‘c’ and ‘k’ of Fig. 2C). Regarding the novel loci, the majority of the identified genes had no GO term associated with them (1110 out of 1359 for *C. intestinalis*, 3184 out of 3337 for *L. planeri*, and 2898 out of 3316 for *X. tropicalis*) (see the ‘Methods’ for GO analysis details). This suggests these novel loci that lack associated GO terms may be taxon-specific or rapidly evolving genes. After performing a GO enrichment analysis on the loci that did have associated GO terms, no GO terms were enriched for *C. intestinalis* or *L. planeri*. However, for *X. tropicalis* we found 209 GO terms significantly enriched (Additional File 1: Table S1), most of them linked to muscle- and heart-related functions, including muscle contraction, structural assembly, and development.

The transcript:gene ratio (t/g ratio) was calculated for the total number of expressed genes and transcripts obtained for each transcriptome, as well as for subsets of particular gene categories (Table 2). We observed a higher number of different transcripts per expressed gene in the vertebrates relative to the invertebrate *Ciona* only for TCF/LEF genes (TCFs), SMADs and GLIs (Fig. 3A).

Table 1 Long-read sequencing reads. Reads obtained after long-read sequencing and after data processing for each sample used. Ci: *Ciona intestinalis*; Lp: *Lampetra planeri*; Xt: *Xenopus tropicalis*; St: developmental stage

Stage	Dev process	Input reads	Clean reads	Min. length	Avg. length	Max. length	Sum. length
Ci_St04	Cleavage	1,466,765	574,175	200	512	4385	293,959,329
Xt_St06	Cleavage	1,615,386	1,374,219	200	897.8	5474	1,233,804,871
Ci_St12	Gastrulation	2,807,191	2,156,039	200	891.2	7527	1,921,535,475
Xt_St10	Gastrulation	2,876,070	2,277,830	200	626.7	3851	1,427,433,920
Ci_St15	Neurulation	860,144	610,643	200	515.4	3441	314,711,689
Ci_St16	Neurulation	1,378,599	839,501	200	668.8	3560	561,488,108
Xt_St16	Neurulation	1,436,005	1,258,985	200	803.8	4049	1,011,971,517
Xt_St20	Neurulation	2,435,888	2,048,749	200	704.8	4483	1,443,978,930
Lp_St22	Post-neurulation	985,970	730,948	200	680.3	5565	497,288,356
Ci_St21	Cell Diff	3,526,232	2,724,082	200	647.3	3230	1,763,334,732
Ci_St26	Cell Diff	2,601,133	1,913,539	200	566.5	4336	1,083,927,850
Lp_St25	Organogenesis	7,505,549	4,919,531	200	536.8	4812	2,640,918,572
Lp_St28	Organogenesis	5,515,552	3,719,539	200	534.1	5,287	1,986,704,869
Xt_St28	Organogenesis	1,871,477	1,424,131	200	555.6	4628	791,301,969
Xt_St35	Organogenesis	2,506,733	1,541,432	200	440.9	2996	679,623,175

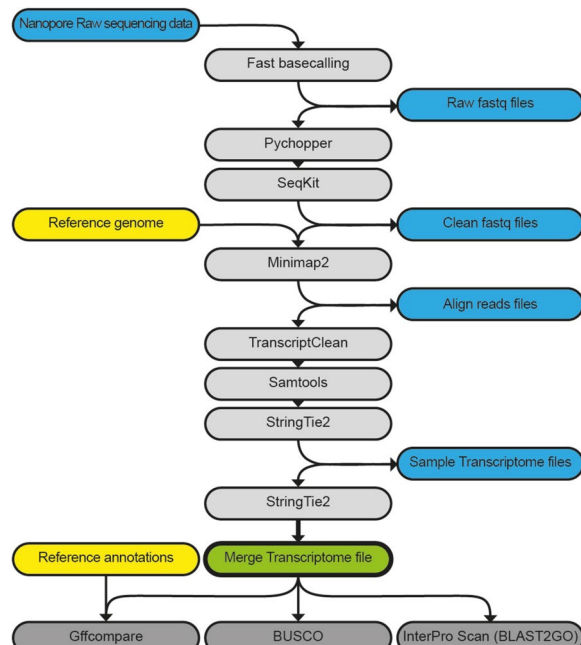


Fig. 1 Pipeline for long-read data processing. Round boxes: files; square boxes: software programmes. Blue boxes: obtained files; yellow boxes: reference files; green box: final transcriptome file; light-grey boxes: software for processing data; dark-grey boxes: software for evaluate quality of obtained transcriptome file

141 Comparisons of the variance of t/g ratio observed on
142 each subset showed that TCFs had a greater variance
143 than most of the other subsets studied ($p\text{-value} < 0.1$,
144 Additional File 1: Tables S2–5), including the subset 'Wnt
145 signalling pathway' (GO:0016055) and the SOX genes,

which belong to the same HMG-box superfamily as the TCF/LEFs. Moreover, a similar pattern was found for SMAD and GLI genes. However, after multiple-test correction, none of these comparisons remained significant (Additional File 1: Table S2). To further assess whether the increase in transcripts observed for these gene families was different from that observed for the other categories, we performed linear regressions for each subset and calculated the regression coefficient (β_1 or slope, Fig. 3B, Additional File 1: Tables S6–8), excluding the t/g ratio of the target gene families from the t/g ratio calculations on the other categories (i.e. All, Over1, Emb. Dev., Wnt path., BMP path., Hh path., and TF, Additional File 1: Table S2). A linear regression model including all individual subsets revealed that the interaction term of GLIs (cell_type_num:SubsetGLIs) and TCFs (cell_type_num:SubsetTCFs) showed significance ($p\text{-value} < 0.01$ and $p\text{-value} < 0.1$, respectively, Additional File 1: Table S6), indicating that the regression coefficient observed for those subsets differed from the reference subset (All).

Next, we performed separate linear regression models for each gene family (TCFs, SMADs, GLIs and SOXs), grouping the remaining subset to increase statistical power. We excluded the Over1 subset, as its high mean increased the regression error, and the pathways subsets not related with the specific gene family, except for SOXs (i.e. TCFs groups: TCFs and All + Emb.Dev.+Wnt path.+TF+SOXs; SMADs groups: SMADs and All + Emb.Dev.+BMP path.+TF+SOXs; GLIs groups: GLIs and All + Emb.Dev.+Hh path.+TF+SOXs; SOXs groups: SOXs and All + Emb.Dev.+Wnt path.+BMP path.+Hh path.+TF). The interaction terms showed

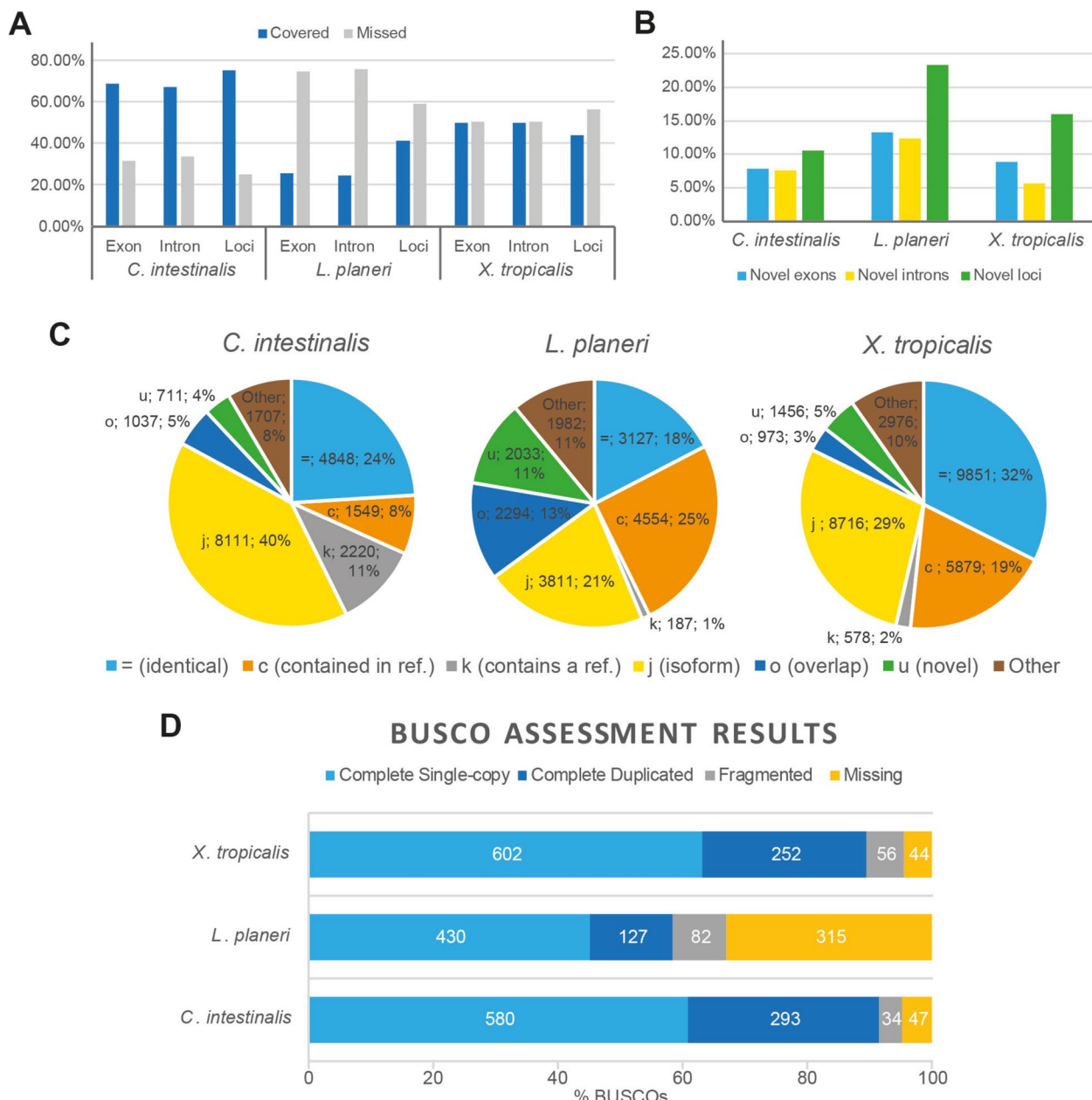


Fig. 2 Transcriptome quality assessments. **A** Covered (blue) and missed (grey) exons/intron/loci for each species data set. **B** Novel exon (blue), intron (yellow), and loci (green) for each species data set. **C** Pie plots showing the distribution of transcript-matching types according to gffcompare categories: = (light-blue), identical reference-query match; c (orange), complete query match within reference; k (grey), complete reference match within query; j (yellow), some splice site mismatch (potential new isoform); o (dark-blue), partial overlapping match; u (green), no match of query within reference (novel); Other (brown), other types of query-reference matches including m (all introns retained), n (some introns retained), e (single exon match), s (intron match on opposite strand), x (exon match on opposite strand), i (contained within reference intron), y (reference contained within intron), p (possible polymerase run-on), and r (repeat). **D** Histogram showing the amount of evolutionary conserved orthologues (BUSCOs) found, as single-copy (light blue), duplicated (dark blue) or fragmented (grey), and missing (yellow)

178 that TCFs, SMADs, and GLIs had a significantly different regression coefficient compared to the grouped sub-179 sets (TCFs $p < 0.01$; SMADs $p < 0.1$; GLIs $p < 0.001$, see 180 Additional File 1: Table S7) whereas SOXs showed no 181

significance (p -value > 0.1 ; Additional File 1: Table S7). 182 This reaffirmed the previously observed pattern for GLIs 183 and TCFs and extended it to SMADs. 184

Table 2 Total number of genes and transcripts for each transcriptome and subsets. All: the whole transcriptome; Over 1: only genes with more than one transcript; Emb. Dev.: genes with the GO term 'Embryo Development' (GO:0009790); Wnt Path.: genes with the GO term 'Wnt Pathway' (GO:0016055); BMP Path.: genes with the GO term 'BMP signalling pathway' (GO:0008101 or GO:0030509); Hh Path.: genes with the GO term 'smoothened signalling pathway' (GO:0007224); TF: genes with the GO term 'DNA-binding transcription factor activity' (GO:0003700); SOXs: SOX genes; TCFs: TCF and TCF/LEF genes; SMADs: SMAD genes; GLIs: GLI genes

	<i>Ciona intestinalis</i>			<i>Lampetra planeri</i>			<i>Xenopus tropicalis</i>		
	Genes	Transcripts	Ratio t/g	Genes	Transcripts	Ratio t/g	Genes	Transcripts	Ratio t/g
All	12,717	20,183	1.59	14,311	17,988	1.26	20,775	30,429	1.46
Over 1	3868	11,171	2.89	2235	5860	2.62	5431	15,105	2.78
Emb. Dev.	15	22	1.47	14	19	1.36	69	106	1.54
Wnt Path	40	58	1.45	29	33	1.14	89	134	1.51
BMP Path	54	86	1.59	37	45	1.22	63	94	1.49
Hh Path	49	90	1.84	43	55	1.28	49	82	1.67
TF	296	481	1.63	130	167	1.28	750	1235	1.65
SOXs	5	7	1.40	3	5	1.67	9	14	1.56
TCFs	1	1	1.00	1	2	2.00	4	9	2.25
SMADs	5	6	1.20	3	4	1.33	7	12	1.71
GLIs	1	1	1.00	1	1	1.00	1	3	3.00

Finally, we performed a linear regression model grouping TCFs, SMADs, and GLIs together as target group, and the remaining subsets (i.e. All, Emb. Dev., Wnt path., BMP path., Hh path., TF and SOXs) as comparison group. The regression coefficient observed for the target group was significantly higher than the one observed for the comparison group (Fig. 3B, Shapiro–Wilk test *p*-values > 0.5; Bartlett test *p*-value < 0.001; Mann–Whitney *U* test: *p*-value < 0.05, Additional File 1: Table S8).

All together, these results indicate that these key developmental transcription factors (TCF/LEFs, SMADs, and GLIs) have a distinctive pattern of a higher number of different transcripts per expressed gene in the vertebrates relative to the invertebrate *Ciona*: in our analysis (summarised in Table 2), TCF/LEFs have 1 gene and 1 transcript in *C. intestinalis* compared to 1 gene and 2 transcripts in *L. planeri* and 4 genes and 9 transcripts in *X. tropicalis*; SMADs have 5 genes and 6 transcripts in *C. intestinalis* compared to 3 genes and 4 transcripts in *L. planeri* and 7 genes and 12 transcripts in *X. tropicalis*; and GLIs have 1 gene and 1 transcript in *C. intestinalis* compared to 1 gene and 1 transcript in *L. planeri* and 1 gene and 3 transcripts in *X. tropicalis* (DNA and Protein sequences available in Additional Data 1–6). Interestingly, the variance observed in the t/g ratio for these three gene families (TCF/LEFs, SMADs, and GLIs) was not significantly different between each of them (*padj* = 1, Additional File 1: Table S2), indicating that they show similar distributions of transcript isoforms per expressed gene within the three chordate groups. Alongside the linear regression modelling that demonstrates a significant increase in t/g ratios of the developmentally expressed

genes in the TCF/LEF, GLI and SMAD families in the two vertebrates relative to the invertebrate *Ciona*, this demonstrates a distinct characteristic of these families relative to other genes found in our transcriptome data.

A new splice isoform in *Ciona intestinalis*

To confirm the transcript sequence and structure of the *C. intestinalis* TCF/LEF (in what was formerly known as *Ciona intestinalis* Type B) relative to the commonly studied sister species *Ciona robusta* (formerly *Ciona intestinalis* type A), we performed RACE-PCR in different stages of development, selected according to the previously described expression of *C. intestinalis* TCF (*CiTCF*) [22]. 5' RACE-PCR was performed in St04 (8-cell; maternal mRNA) and St12 (mid-Gastrula; zygotic mRNA), and 3' RACE-PCR was performed for St04, St12, St16 (late Neurula), and St21 (mid-Tailbud I).

For 5' RACE-PCR, only one fragment was amplified, matching the described gene model. For 3' RACE-PCR two different 3' ends were found. The first was found in all the assessed stages and matched the previously described gene model. The second, smaller in size, was found in St16 and matched the described gene model but with a different final exon. Further analysis of the genomic region between exon 12 and exon 13 in *C. intestinalis* (intron 12; Fig. 4A) showed the presence of this new exon flanked by two transposable elements, partially overlapping one at the 3' end. These transposable elements matched in sequence the previously described miniature inverted-repeat transposable elements (MITE) Cimi-1 [23]. Comparison of intron 12 between *C. robusta* and *C. intestinalis* revealed that

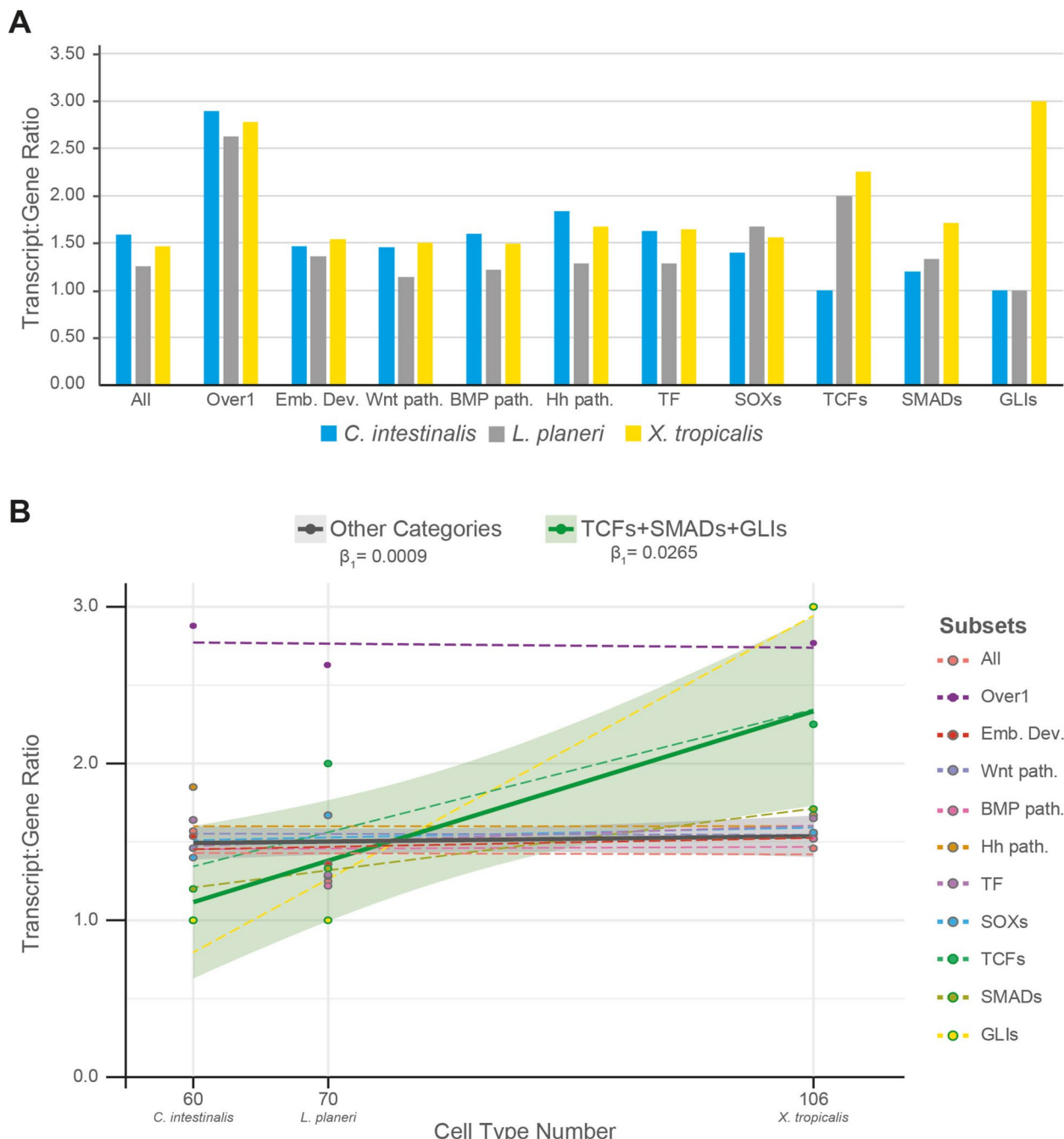


Fig. 3 Transcript:gene ratio. **A** Histogram of the transcript:gene ratios (t/g ratio) for each species (blue: *Ciona intestinalis*; grey: *Lampetra planeri*; yellow: *Xenopus tropicalis*) and category (All: whole transcriptome; Over 1: genes with more than one transcript; Emb. Dev: genes with the GO term 'Embryo Development' (GO:0009790); Wnt path.: genes with the GO term 'Wnt signalling pathway' (GO:0016055); BMP path.: genes with the GO term 'BMP signalling pathway' (GO:0008101 or GO:0030509); Hh path.: genes with the GO term 'smoothened signalling pathway' (GO:0007224); SOXs: SOX genes; TF: genes with the GO term 'DNA-binding transcription factor activity' (GO:0003700); TCFs: TCF and TCF/LEF genes; SMADs: SMAD genes; GLIs: GLI genes). **B** Linear regressions of each subset studied (dotted lines) and for the two groups used for the Mann–Whitney *U* test (solid lines): 'Other categories' encompassing All, Emb. Dev., Wnt path., BMP path., Hh path., TF and SOXs (grey line), and 'TCFs + SMADs + GLIs' encompassing those three gene families (green line). The t/g ratio is plotted against the cell type number in development for each species, according to Cao et al.⁴⁶ for *Ciona*, Pang et al.⁴⁷ for lamprey, and Liao et al.⁴⁸ for *Xenopus*. Dots: Transcript:Gene ratio values. Dot outline: belonging to group, 'TCFs + SMADs + GLIs' (green) or 'Other categories' (grey). β_1 : regression coefficient

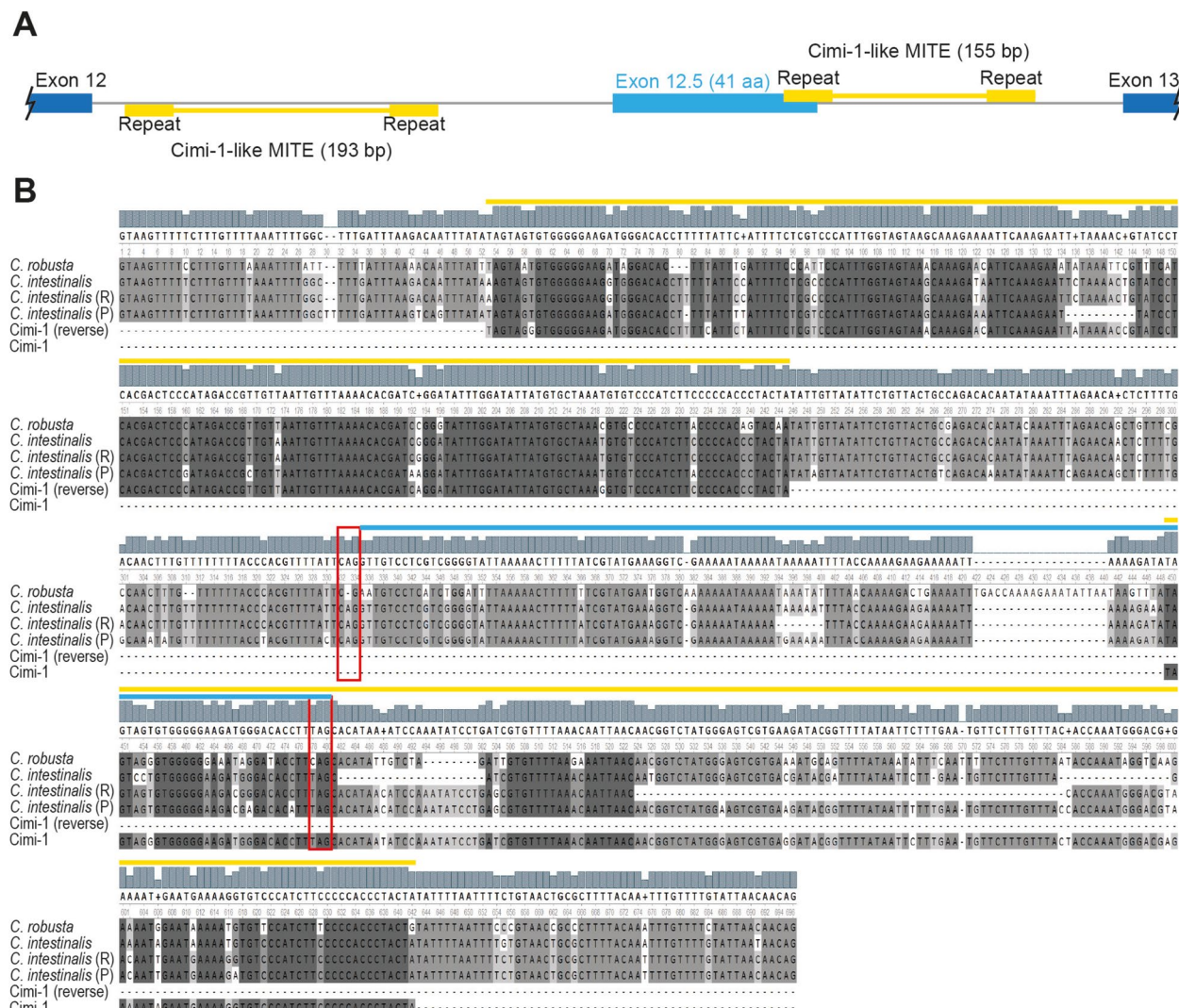


Fig. 4 Schematic of *CiTCF* intron 12. **A** Schematic of the *C. intestinalis* genomic region where exon 12.5 is found. **B** DNA alignment of *TCF* intron 12 of *C. intestinalis* and *C. robusta*. *C. intestinalis* (R): sequence from Roscoff reference genome (GCA_018327825.1); *C. intestinalis* (P): sequence from Plymouth reference genome (GCA_018327805.1); dark blue: annotated exons; light blue: new exon (exon 12.5); yellow: Cimi-1-like sequences; red boxes: acceptor site and stop codon of exon 12.5

248 despite the Cimi-1 insertions being conserved, this was
249 not the case for the splice acceptor site nor the stop
250 codon of exon 12.5 (Fig. 4B), indicating that this newly
251 discovered exon may be specific to *C. intestinalis*. To
252 confirm this alternative C-terminus, we designed a
253 specific Reverse primer for exon 12.5 and performed
254 RT-PCRs on St12, St15 (mid-Neurula) and St21. This
255 isoform was found only in post-gastrulation stages. *C.*
256 *intestinalis* thus produces two isoforms of TCF/LEF, in
257 contrast to the single isoform produced by this gene in
258 *C. robusta*.

Discussion

Our transcriptome analyses focused on gene expression during embryo development and organogenesis revealed that *TCF/LEF*, *SMAD* and *GLI* genes exhibit a distinctive pattern of higher numbers of splice isoforms per developmentally expressed gene in vertebrates than the representative from the closest invertebrate sister group, represented here by the urochordate *C. intestinalis*. This larger number of splice isoforms occurs in addition to the increase in parologue numbers in these transcription factors at the origin of vertebrates.

270 Our previous in silico analyses identified an increase
 271 in TCF/LEF gene number encoded in the genome at
 272 the invertebrate-to-vertebrate transition, likely via the
 273 whole genome duplications that occurred early in vertebrate
 274 evolution, and in addition suggested there was an increase in isoform diversity in this gene family [21].
 275 However, this diversity remained to be quantified. It also
 276 remained to be determined as to when these isoforms are
 277 expressed during development and hence are presumably
 278 functional. This analysis is provided here. Another
 279 important question was whether the evolutionary patterns
 280 seen in this major transcriptional effector of the
 281 cWnt signalling pathway were unique, or also occurred
 282 elsewhere, especially in other major developmental
 283 signalling pathways like Hh and BMP/TGF β .
 284

285 Invertebrates typically have four SMADs, corresponding
 286 to a single-copy of each SMAD subgrouping (common
 287 SMAD (Co-SMAD), inhibitory SMAD (I-SMAD),
 288 BMP-regulated receptor SMAD (R-SMAD) and TGF β -
 289 regulated R-SMAD). However, *Ciona* has independently
 290 duplicated the TGF β -regulated R-SMAD [24], giving a
 291 total of five SMADs in this tunicate. Meanwhile vertebrates
 292 usually possess eight different SMADs (one Co-
 293 SMAD, two I-SMADs, three BMP-regulated R-SMADs,
 294 and 2 TGF β -regulated R-SMADs) [25, 26]. In the GLI
 295 family, invertebrates have a single GLI gene while vertebrates
 296 typically have three paralogues [27]. Thus, the SMAD and GLI
 297 families show a similar pattern of
 298 increased parologue numbers encoded by the genome to
 299 that seen in the TCF/LEF family. However, the amount
 300 of developmentally expressed splice isoform diversity
 301 remained to be analysed for both SMAD and GLI families.
 302 Our data demonstrate that these families, when analysed
 303 by linear regression modelling against numbers of
 304 cell types in these chordates, show a similar pattern to
 305 the TCF/LEF family, with a significantly higher number
 306 of isoforms per developmentally expressed gene in the
 307 vertebrates we studied relative to the invertebrate sister
 308 group.

309 It is striking that this invertebrate-to-vertebrate pattern
 310 for the TCF/LEF, SMAD and GLI genes is significantly
 311 different from other developmentally expressed
 312 genes and their transcripts found in our new transcrip-
 313 tomes ('All' category in Fig. 3). This is also the case when
 314 we focus on genes that demonstrably exhibit alternative
 315 splicing (that is, have more than one transcript per gene:
 316 the 'Over 1' category in Fig. 3), in which the *C. intestinalis*
 317 ratio is indistinguishable from those of the two vertebrates.
 318 Thus, there is not simply a general increase in
 319 isoform diversity in developmentally expressed genes at
 320 the invertebrate-to-vertebrate transition. Since these first
 321 two categories encompass genes that span a variety of
 322 biological functions, we also focused on genes thought

323 to be more specifically involved in embryo development,
 324 in case there is a general increase in complexity of develop-
 325 mental control genes associated with the invertebrate-
 326 to-vertebrate transition and the evolution of vertebrate
 327 complexity. No distinct pattern was observed between
 328 the invertebrate *C. intestinalis* and the vertebrates. This
 329 lack of invertebrate to vertebrate distinction was also
 330 observed when the focus was even more specific, onto
 331 Wnt pathways as a whole (Fig. 3). Another alternative
 332 possibility was explored by comparison to Transcrip-
 333 tion Factors in general ('TF' in Fig. 3) in case the mediators
 334 of transcriptional control are the focus of change
 335 between invertebrates and vertebrates. No significant
 336 distinction was found. As a final test of how distinct the
 337 pattern found for the TCF/LEF family was, we analysed
 338 the SOX genes, since these are in the same superfamily
 339 as the TCF/LEF genes and hence act as the closest com-
 340 parison possible. The invertebrate-to-vertebrate pattern
 341 for the TCF/LEF genes is significantly different to that of
 342 the SOX genes. Thus, the TCF/LEF genes stand-out from
 343 all of these different categories of genes, implying a spe-
 344 cific expansion in the splice isoform diversity focused on
 345 these transcription factor mediators of the cWnt path-
 346 way. Notably, the only categories of genes that we found
 347 with comparable invertebrate-to-vertebrate patterns
 348 were those of the transcription factor mediators of other
 349 major intercellular signalling pathways (the SMAD and
 350 GLI genes).

351 Amongst all of this vertebrate genetic diversity, it has
 352 been shown that vertebrate TCF/LEF paralogues and
 353 GLI paralogues have some degree of redundancy at
 354 the functional level [17, 28]. Nevertheless, there is also
 355 evidence that different TCF/LEF isoforms can target
 356 different genes [29], showing both sub- and neo-functionalisation.
 357 Similarly, GLI isoforms have been shown to have opposing roles activating or repressing the gene
 358 expression of their specific target genes [28]. Therefore,
 359 the diversity of vertebrate genes in TCF/LEF, SMAD and
 360 GLI families, and the isoforms produced from them, pre-
 361 sumably reflects a wide array of functional capabilities
 362 downstream of important developmental signalling path-
 363 ways in vertebrates.

364 These three gene families are the main transcription
 365 factor effectors of major intercellular signalling path-
 366 ways (cWnt, BMP/TGF β and Hh, respectively), which
 367 are integral to embryo development, organogenesis and
 368 homeostasis. Their major roles in development in con-
 369 junction with the correlation of isoform diversity with
 370 organism complexity [1–4] is consistent with the hypoth-
 371 esis that increased diversity of these transcription factors
 372 may be making a disproportionate contribution to the
 373 evolution of vertebrate complexity relative to inver-
 374 tebrates. Interestingly, previous studies had observed

376 genes resulting from duplication usually retain lower
 377 numbers of isoforms, with duplication and isoform diversity
 378 being inversely correlated evolutionary patterns
 379 [30, 31]. This makes the pattern observed here in these
 380 developmental signalling transcription factor effectors
 381 even more striking, as our data shows that *TCF/LEF*,
 382 *SMAD* and *GLI* genes are exceptions to this inverse
 383 correlation. This could be an indicator of a significant role
 384 for isoform diversity of these key transcription factors in
 385 the evolutionary origins and diversification of vertebrate
 386 complexity.

387 One caveat to this hypothesis is whether the species
 388 selected here are good representatives of the inverte-
 389 brate-to-vertebrate transition. *C. intestinalis*, for exam-
 390 ple, was selected because it is a urochordate and as such
 391 is a member of the closest invertebrate clade to the ver-
 392 tebrates, and is also accessible and amenable to gene
 393 expression and developmental experimentation. There
 394 are, however, aspects of its genome organisation and
 395 content that are relatively derived within the chordates
 396 [32]. Also, it is known that amphioxus exhibits alter-
 397 native splicing from its *Gli* gene, producing two distinct
 398 isoforms [33], rather than the single isoform of *Ciona*
 399 *GLI* that was found here. It is also notable that our analy-
 400 ses are focused on the transcripts found within our new
 401 transcriptome data. While this enhances comparability
 402 between the different species, we are not necessarily cap-
 403 turing all isoforms produced by each of the three species
 404 selected. Rare transcripts expressed at very low levels in
 405 embryogenesis, or transcripts expressed only in adult
 406 stages, will not be present in our data. These are areas for
 407 future further work, to quantify the patterns described
 408 here with even greater precision. Nevertheless, there is
 409 no indication that the three transcription factor families
 410 focused on here are unusual in *Ciona* relative to inverte-
 411 brates in general in any major way, but this is also an area
 412 for further scrutiny in the future, particularly as addi-
 413 tional high-quality genome assemblies and more long-
 414 read transcriptome data becomes available.

415 In addition to these 'signalling transcription factor'
 416 findings, the long-read transcriptomes provided in this
 417 work are also a valuable resource for deeper understand-
 418 ing of gene expression during embryo development of
 419 different chordates, including species not previously
 420 assessed with long-read transcriptome sequencing, such
 421 as Cyclostomata and Urochordata. However, despite all
 422 the samples being processed in the same way and our
 423 obtaining similar quality values within urochordate and
 424 gnathostome data sets, the quality of the cyclostome data
 425 set was not as good (Fig. 2). This issue could be due to the
 426 GC-richness of cyclostome genomes [34] and/or the fact
 427 that *L. planeri* (the species sampled) and *P. marinus* (the
 428 species used as the lamprey reference genome) are more

429 evolutionarily distant and distinct than the species used
 430 for urochordates (samples of *C. intestinalis* and reference
 431 genome of *C. robusta*) and gnathostomes (samples and
 432 reference genome of *X. tropicalis*).
 433

434 It is also notable that for *C. intestinalis*, the transcript
 435 type category that had the highest number of transcripts
 436 was 'j' (40%, Fig. 2C), showing that most of the trans-
 437 scripts had mismatched splicing sites (junctions) against
 438 reference annotations. This could be an indicator of
 439 potential novel isoforms found in this new *C. intestinalis*
 440 transcriptome data for previously annotated genes in *C.*
 441 *robusta*. In fact, our finding of an alternative transcript of
 442 *CiTCF* is the first evidence that *C. intestinalis* has more
 443 than one TCF isoform. However, this second transcript
 444 of *CiTCF* was only found by RACE-PCR rather than
 445 being in the transcriptome data, which may reflect the
 446 RACE-PCR having higher sensitivity than cDNA long-
 447 molecule sequencing, since the PCR is gene-specific. In
 448 addition, the partial overlap of exon 12.5 with the Cimi-1
 449 MITE sequence provides an example of how transposable
 450 elements can alter intronic sequences that then provide
 451 material for the evolutionary origin of novel exons, in
 452 this case in concert with point mutations that generated a
 453 new splice acceptor site as well as a new stop codon.

Conclusions

454 We have created de novo transcriptomes of embryo
 455 development for three different chordates: *C. intesti-*
 456 *nalis* (Urochordata), *L. planeri* (Cyclostomata) and *X.*
 457 *tropicalis* (Gnathostomata). Our analyses demonstrate
 458 distinctive increases in isoform diversity at the inverte-
 459 brate-to-vertebrate transition specifically among trans-
 460 cription factor effectors of key intercellular signalling
 461 pathways that drive cell type diversity. This distinctive
 462 change focused on these specific gene families (TCF/
 463 LEF, SMAD and GLI) goes beyond the previous observa-
 464 tions of a general correlation between increased isoform
 465 diversity and evolution of animal complexity. This dem-
 466 onstrates likely disproportionate roles for these specific
 467 transcription factor families in the evolution of verte-
 468 brate complexity, which needs to be explored with future
 469 functional assays of these various isoforms.

Methods

Material fixation and RNA extraction

470 After in vitro fertilisation, selected embryological stages
 471 from *C. intestinalis*, *L. planeri* and *X. tropicalis* were fixed
 472 in RNAlater™ (Invitrogen, AM7021) for a minimum of
 473 16 h at 4 °C, taking care that the amount of RNAlater™
 474 was at least 10 times the volume of the sample. Stage
 475 numbering was done according to Hotta [35], Tahara
 476 [36] and Zahn [37]. RNA extractions were performed
 477 with 'RNAeasy mini kit' (QIAGEN, 74,104) following the
 478

480 manufacturer's protocol. The quality and quantity of the
 481 total RNA obtained was tested by gel electrophoresis and
 482 Nanodrop spectrophotometer.

483 **cDNA long-read sequencing**

484 For each sample analysed, 50 ng of total RNA was pro-
 485 cessed using the PCR-cDNA Barcoding Kit (Oxford
 486 Nanopore Technologies (ONT), SQK-PCB109). The first
 487 strand synthesis was performed following the manufac-
 488 turer's instructions (Thermo Scientific Maxima H Minus
 489 First Strand cDNA Synthesis Kit with dsDNase, K1681).
 490 First, a previous DNase treatment of the total RNA was
 491 performed as follows: incubation of 10 min at 37 °C fol-
 492 lowed by an inactivation of 5 min at 55 °C in the presence
 493 of 10 mM of DTT. After, the sample was cooled on ice
 494 and VN Primers and dNTPs were added. After mixing,
 495 the sample was incubated 5 min at 65 °C and snap cooled
 496 on a pre-chilled freezer block. Then, 5xRT buffer, Strand-
 497 Switching Primers and Maxima H Minus Enzyme Mix
 498 were added and the sample was mixed by pipetting. The
 499 reverse transcription (RT) reaction was performed by
 500 incubating the sample 10 min at 25 °C followed by 92 min
 501 at 42 °C and 5 min at 85 °C.

502 A single PCR reaction was performed for each RT reaction.
 503 The PCR reaction was prepared according to the
 504 PCR-cDNA Barcoding Kit protocol with minor modi-
 505 fications in the cycling conditions: initial denaturation
 506 at 95 °C for 30 s; 18 cycles of denaturation at 95 °C for
 507 10 s, annealing at 62 °C for 20 s, extension at 65 °C for
 508 2 min 30 s; final extension of 65 °C for 10 min and hold
 509 at 4 °C. Each reaction was treated with Exonuclease I
 510 (New England Biolabs, M0293) followed by a purification
 511 with AMPure XP beads (Beckman Coulter, A63880) as
 512 indicated in the PCR-cDNA Barcoding Kit protocol with
 513 minor modification (i.e. we used 30 µL of AMPure XP
 514 beads per PCR reaction). The concentration and quality
 515 of the obtained samples were assayed by Nanodrop and
 516 gel electrophoresis. The sequencing was performed with
 517 a maximum of 100 fmol per run.

518 MinION flow cells (ONT, FLO-MIN106D) underwent
 519 flow cell check prior to library construction. The bar-
 520 coded PCR-cDNA libraries were prepared for sequencing
 521 and the MinION flow cell was primed using the flow cell
 522 priming kit (ONT, EXP-FLP002) as indicated in the PCR-
 523 cDNA Barcoding Kit protocol. A maximum of six PCR-
 524 cDNA libraries per run were sequenced in parallel on a
 525 single MinION flow cell with Min-KNOWN software
 526 v.21.02.2 (ONT). Fast basecalling was performed in real-
 527 time with a maximum data acquisition time of 48 h and
 528 the following filters applied: minimum Barcode score of
 529 60 and minimum Qscore of 7. All the raw data produced
 530 is available at the Sequence Read Archive (SRA) database

531 under accession numbers SRR24756885-SRR24756899,
 532 BioProject PRJNA977127.

533 **Transcriptomic data processing**

534 The cDNA ONT reads were pre-processed with pycrop-
 535 per (ONT), to remove the primer sequences intro-
 536 duced by the protocol, and with SeqKit [38], to remove
 537 sequences under 200 bp length. Each cDNA ONT
 538 library for each developmental stage sequenced was
 539 aligned to the corresponding reference genome by mini-
 540 map2 [39] (*C. intestinalis* reads aligned against *Ciona*
 541 *robusta* genome (GCA_000224145.2 [40]); *L. plan-*
 542 *eri* reads aligned against *Petromyzon marinus* genome
 543 (GCA_010993605.1 [41]); *X. tropicalis* reads aligned
 544 against *X. tropicalis* genome (GCA_000004195.3 [42])),
 545 transcripts refined with TranscriptClean [43] and anno-
 546 tated with StringTie2 [44] software. Finally, the stage-spe-
 547 cific annotations were merged into a general annotation
 548 file for each species with StringTie2 '-merge' option and
 549 reference transcriptome and proteome dataset were gen-
 550 erated using TransDecoder [45]. The obtained proteome
 551 datasets and general annotation file were analysed with
 552 BUSCO [46] (v5.2.2) and gffcompare [47], respectively, to
 553 assess the quality of the transcriptomes. For obtaining the
 554 GO annotations, the InterPro Scan option of Blast2GO
 555 software (v.6.0.3) and the EggNOG-mapper tool [48]
 556 were run using each transcriptome dataset as input.

557 **Statistical analysis**

558 The GO enrichment analysis was done separately for
 559 each species. The analysis was performed in R using the
 560 function 'enricher()' from the 'clusterProfiler' package
 561 providing as inputs the list of 'u' genes and the GOs and
 562 genes found in the whole transcriptome.

563 For each species dataset, the ratio transcript:gene (t/g
 564 ratio) for developmentally expressed genes was calcu-
 565 lated for all the genes present in the created transcripto-
 566 me (All), genes that had more than 1 transcript (Over
 567 1), genes with the gene ontology numbers GO:0009790
 568 (Embryo Development, Emb. Dev.), GO:0016055
 569 (Wnt signalling pathway, Wnt path.), GO:0008101 or
 570 GO:0030509 (BMP signalling pathway, BMP path.),
 571 GO:0007224 (smoothened signalling pathway, Hh path.)
 572 and GO:0003700 (DNA-binding transcription factor
 573 activity, TF), and for the gene families SOXs, TCFs,
 574 SMADs and GLIs. For the target gene families a BLASTN
 575 against the raw reads data was done to ensure isoform
 576 detection. We performed F-tests (or Bartlett's test when
 577 data not normal by Shapiro Wilk test) to compare the
 578 variances of t/g ratios within the different subsets (i.e.
 579 All, Over 1, Emb. Dev., Wnt path., BMP path., Hh path.,
 580 TF, SOXs, TCFs, SMADs and GLIs) doing pairwise com-
 581 parisons and Bonferroni correction for multiple-test

582 comparisons (Additional File 1: Table S2). A difference in
 583 the variance was expected when the t/g ratio was noticeably
 584 different within species. The regression coefficient
 585 (β_1) for each subset was estimated using a linear regression
 586 model with t/g ratio values and species complexity
 587 defined as the number of cell types detected by single-cell
 588 RNAseq in larva/organogenesis stage (*C. intestinalis* [49]:
 589 60; *L. planeri* [50]: 70; *X. tropicalis* [51]: 106). Finally, a
 590 Mann-Whitney *U* test was applied to evaluate differences
 591 in regression coefficients between groups. In all
 592 cases, data normality was assessed by Shapiro-Wilk tests
 593 (see Additional File 1: Tables S2 and S8).

594 RACE-PCR, cloning and sequencing

595 Total RNA of *C. intestinalis* was used for 3' RACE and
 596 5' RACE experiments using FirstChoice™ RLM-RACE
 597 Kit (Invitrogen, AM1700) following the manufacturer's
 598 protocol and with the following CiTCF-specific primers:
 599 5'-CAGGCATGTTACGATAACCATATCCA-3'
 600 (3' RACE), 5'-CATCACAATTACATCCACATCTG
 601 GTGGT-3' (5' RACE), 5'-CTTCACATATGGCCG
 602 ACTTGGTTGTCACCT-3' (nested 3' RACE) and
 603 5'-TCGCGTTCTTGAACCAGGTTCAG-3' (nested
 604 5' RACE). PCRs were performed with Taq DNA poly-
 605 merase (Thermo Scientific, EP0402) following the man-
 606 ufacturer's protocol and results were assessed by gel
 607 electrophoresis in 1% agarose gels.

608 The individual bands obtained after nested RACE-
 609 PCR were purified with the ISOLATE II PCR and Gel Kit
 610 (Meridian Bioscience, BIO-52059), and cloned with the
 611 pGEM®-T Easy Vector System (Promega, A1360), follow-
 612 ing the manufacturer's protocol. Transformation was per-
 613 formed into *E. coli* competent cells (Agilent, XL10-Gold
 614 Ultracompetent cells, 200,314) by heat-shock. All clones
 615 were selected by Ampicillin resistance and their compo-
 616 sition was confirmed by enzyme digestion with NotI (New
 617 England Biolabs, R0189) and Sanger sequencing (Oxford
 618 Zoology service, Eurofins service). The sequences were
 619 compared against *C. intestinalis* genomic sequences from
 620 Roscoff reference genome (GCA_018327825.1 [52]) and
 621 from Plymouth reference genome (GCA_018327805.1
 622 [53]).

623 The intronic region within exon 12 and exon 13 of *C.*
 624 *intestinalis* TCF was amplified with the following primer
 625 pair: 5'-TCGCACGATAATGTTAACAGC-3' (forward
 626 primer), 5'-GTTCATAGCTACTTGATGGTTGGA-3'
 627 (reverse primer). Specific exon 12.5 PCRs were done with
 628 the following primer pair: 5'-ACAACAGCAATTATG
 629 GTGCGCAC-3' (forward primer), 5'-ATACCCGACG
 630 AGGACAAC-3' (reverse primer). The protocols for PCR
 631 and posterior cloning were as described above.

632 Abbreviations

633 BLAST Basic Local Alignment Search Tool

BMP	Bone morphogenetic protein	634
BUSCO	Benchmarking Universal Single-Copy Orthologs	635
cDNA	Complementary deoxyribonucleic acid	636
dNTPs	Deoxyribonucleotide triphosphates	637
DTT	Dithiothreitol	638
GLI	Glioma-Associated Oncogene	639
GO	Gene Ontology	640
Hh	Hedgehog	641
HMG box	High Mobility Group box	642
MITE	Miniature inverted-repeat transposable elements	643
RACE PCR	Rapid Amplification of cDNA Ends Polymerase Chain Reaction	644
RNA	Ribonucleic acid	645
RT PCR	Reverse transcription polymerase chain reaction	646
SMAD	Small/Mothers Against DPP Homolog	647
SOX	SRY-related HMG box	648
TCF/LEF	T-cell factor/lymphoid enhancer factor	649
TGF β	Transforming growth factor β	650

594 Supplementary Information

595 The online version contains supplementary material available at <https://doi.org/10.1186/s12915-026-02522-w>.

Additional file 1: Tables S1-8. Table S1. GO terms enriched in the novel loci found in our transcriptomic data of <i>Xenopus tropicalis</i> . Table S2. P-values of F-test or Bartlett's tests performed on each group, according to the Shapiro-Wilk test p-values. Table S3. Gffcompare results of <i>X. tropicalis</i> transcriptome, including the GO terms found for each gene ID (qry_gene_id). Table S4. Gffcompare results of <i>L. planeri</i> transcriptome, including the GO terms found for each gene ID (qry_gene_id). Table S5. Gffcompare results of <i>C. intestinalis</i> transcriptome, including the GO terms found for each gene ID (qry_gene_id). Table S6. Linear regression model with individual subsets. The subset 'All' is used as reference for the p-value calculations. Table S7. Linear regression model summaries for each studied subset. Table S8. Regression coefficients obtained from each linear regression performed. Data normality assessed with Shapiro-Wilk test, data homogeneity assessed with Bartlett's test, difference of means assessed with Mann-Whitney U Test. SD: standard deviation.	654
	655
	656
	657
	658
	659
	660
	661
	662
	663
	664
	665
	666
	667
	668
Additional file 2. Data 1-6. DNA and protein sequences for the TCF/LEF, GLI, and SMAD families found in the transcriptomes reported here.	669
	670

604 Acknowledgements

605 We thank members of the Ferrier and Hoppler labs for discussions related to
 606 this work. We also thank the harbour-masters at Arbroath harbour for always
 607 readily allowing us access for collecting *Ciona*.

608 Authors' contributions

609 N.P.T.A. led the experiments and analyses as well as writing the manuscript.
 610 M.S. provided **X. tropicalis** material and contributed to the writing. S.M.S.
 611 provided **L. planeri** material and advice on analyses and manuscript writing.
 612 S.H. obtained funding, co-supervised the research, and contributed to analyses
 613 and manuscript writing. D.E.K.F. obtained funding, supervised the research,
 614 and contributed to analyses and manuscript writing. All authors read and
 615 approved the final manuscript.

616 Funding

617 This work was supported by the Biotechnology and Biological Sciences
 618 Research Council (BBSRC), linked project references BB/S016856/1 and BB/
 619 S020640/1. NPTA has received funding from the postdoctoral fellowship
 620 programme Beatriu de Pinós (2021 BP 00067), funded by the Secretary of
 621 Universities (Government of Catalonia) and by the Horizon 2020 programme of
 622 research and innovation of the European Union under the Marie Skłodowska-
 623 Curie grant agreement No 801370.

624 Data availability

625 All the raw data produced is available at the Sequence Read Archive (SRA)
 626 database under accession numbers SRR24756885-SRR24756899, BioProject
 627 PRJNA977127. GO terms found for each transcriptome are included in the
 628 Additional File 1: Tables S3-5.

696

Declarations

697

Ethics approval and consent to participate

698

Lamprey embryos were collected under Forestry England permit 024225/2022. Embryo culture was conducted under ethical approval by the AWERB of the Department of Zoology, University of Oxford. For *Xenopus* experiments conducted at the University of Aberdeen, all animal experiments were carried out under license from the United Kingdom Home Office (Establishment Licence: X6A11A5D0, Project Licence: PPL PA66BEC8D, Personal Licence: I34544403).

699

700

701

702

703

704

705

Consent for publication

706

Not applicable.

707

708

709

710

Competing interests

711

The authors declare no competing interests.

712

Received: 23 May 2025 Accepted: 16 January 2026

713

714

715

716

717

718

719

720

721

722

723

724

725

726

727

728

729

730

731

732

733

734

735

736

737

738

739

740

741

742

743

744

745

746

747

748

749

750

751

752

753

754

755

756

757

References

1. Adami C. What is complexity? *Bioessays*. 2002;24:1085–94. <https://doi.org/10.1002/bies.10192>.
2. Hahn MW, Wray GA. The g-value paradox. *Evol Dev*. 2002;4:73–5. <https://doi.org/10.1046/j.1525-142X.2002.01069.x>.
3. Bush SJ, Chen L, Tovar-Corona JM, Urrutia AO. Alternative splicing and the evolution of phenotypic novelty. *Philos Trans R Soc Lond B Biol Sci*. 2017;372:20150474. <https://doi.org/10.1098/rstb.2015.0474>.
4. Yang P, Wang D, Kang L. Alternative splicing level related to intron size and organism complexity. *BMC Genomics*. 2021;22:853. <https://doi.org/10.1186/s12864-021-08172-2>.
5. Klingel S, Morath I, Strietz J, Menzel K, Holstein TW, Grädl D. Subfunctionalization and neofunctionalization of vertebrate Lef/Tcf transcription factors. *Dev Biol*. 2012;368:44–53. <https://doi.org/10.1016/j.ydbio.2012.05.012>.
6. Marlétaz F, Firbas PN, Maeso I, Tena JJ, Bogdanovic O, Perry M, et al. Amphioxus functional genomics and the origins of vertebrate gene regulation. *Nature*. 2018;564:64–70. <https://doi.org/10.1038/s41586-018-0734-6>.
7. Chen L, Bush SJ, Tovar-Corona JM, Castillo-Morales A, Urrutia AO. Correcting for differential transcript coverage reveals a strong relationship between alternative splicing and organism complexity. *Mol Biol Evol*. 2014;31:1402–13. <https://doi.org/10.1093/molbev/msu083>.
8. Hoppler S, Moon RT, editors. *Wnt Signaling in Development and Disease*. Hoboken, NJ, USA: John Wiley & Sons, Inc; 2014. <https://doi.org/10.1002/9781118444122>.
9. Steinhart Z, Angers S. Wnt signaling in development and tissue homeostasis. *Development*. 2018. <https://doi.org/10.1242/dev.146589>.
10. Mayer C-D, Giclais SM de La, Alsehly F, Hoppler S. Diverse LEF/TCF Expression in Human Colorectal Cancer Correlates with Altered Wnt-Regulated Transcriptome in a Meta-Analysis of Patient Biopsies. *Genes (Basel)*. 2020;11. <https://doi.org/10.3390/genes11050538>.
11. Pradas-Juni M, Nicod N, Fernández-Rebolledo E, Gomis R. Differential transcriptional and posttranslational transcription factor 7-like 2 regulation among nondiabetic individuals and type 2 diabetic patients. *Mol Endocrinol*. 2014;28:1558–70. <https://doi.org/10.1210/me.2014-1065>.
12. Bem J, Brožko N, Chakraborty C, Lipiec MA, Koziński K, Nagalski A, et al. Wnt/β-catenin signaling in brain development and mental disorders: keeping TCF7L2 in mind. *FEBS Lett*. 2019;593:1654–74. <https://doi.org/10.1002/1873-3468.13502>.
13. Akiyama T, Raftery LA, Wharton KA. Bone morphogenetic protein signaling: the pathway and its regulation. *Genetics*. 2023. <https://doi.org/10.1093/genetics/iyad200>.
14. Jing J, Wu Z, Wang J, Luo G, Lin H, Fan Y, et al. Hedgehog signaling in tissue homeostasis, cancers and targeted therapies. *Signal Transduct Target Ther*. 2023;8:315. <https://doi.org/10.1038/s41392-023-01559-5>.
15. Xu J, Iyyanar PPR, Lan Y, Jiang R. Sonic hedgehog signaling in craniofacial development. *Differentiation*. 2023;133:60–76. <https://doi.org/10.1016/j.diff.2023.07.002>.
16. Croce JC, Holstein TW. The Wnt's Tale. In: *Wnt Signaling in Development and Disease*. Hoboken, NJ, USA: John Wiley & Sons, Inc; 2014. p. 161–76. <https://doi.org/10.1002/9781118444122.ch12>.
17. Hoppler S, Kavanagh CL. Wnt signalling: variety at the core. *J Cell Sci*. 2007;120:385–93. <https://doi.org/10.1242/jcs.03363>.
18. Mao CD, Byers SW. Cell-context dependent TCF/LEF expression and function: alternative tales of repression, de-repression and activation potentials. *Crit Rev Eukaryot Gene Expr*. 2011;21:207–36. <https://doi.org/10.1615/CritRevEukarGeneExpr.v21.i10>.
19. Cadigan KM, Waterman ML. TCF/LEFs and Wnt signaling in the nucleus. *Cold Spring Harb Perspect Biol*. 2012;4:a007906–a007906. <https://doi.org/10.1101/cshperspect.a007906>.
20. Hoppler S, Waterman ML. Evolutionary Diversification of Vertebrate TCF/LEF Structure, Function, and Regulation. In: *Wnt Signaling in Development and Disease*. Hoboken, NJ, USA: John Wiley & Sons, Inc; 2014. p. 225–37. <https://doi.org/10.1002/9781118444122.ch17>.
21. Torres-Aguila NP, Salonna M, Hoppler S, Ferrier DEK. Evolutionary diversification of the canonical Wnt signaling effector TCF/LEF in chordates. *Dev Growth Differ*. 2022. <https://doi.org/10.1111/dgd.12771>.
22. Garstang MG, Osborne PW, Ferrier DEK. TCF/Lef regulates the Gsx parahox gene in central nervous system development in chordates. *BMC Evol Biol*. 2016;16:57. <https://doi.org/10.1186/s12862-016-0614-3>.
23. Simmen MW, Bird A. Sequence analysis of transposable elements in the sea squirt, *Ciona intestinalis*. *Mol Biol Evol*. 2000;17:1685–94. <https://doi.org/10.1093/oxfordjournals.molbev.a026267>.
24. Dehal P, Satoh Y, Campbell RK, Chapman J, Degnan B, De Tomaso A, et al. The draft genome of *Ciona intestinalis*: insights into chordate and vertebrate origins. *Science*. 2002;298:2157–67. <https://doi.org/10.1126/science.1080049>.
25. Attisano L, Tuen Lee-Hoefflich S. The smads. *Genome Biol*. 2001;2:reviews3010.1. <https://doi.org/10.1186/gb-2001-2-8-reviews3010>.
26. Massagué J, Seoane J, Wotton D. Smad transcription factors. *Genes Dev*. 2005;19:2783–810. <https://doi.org/10.1101/gad.135075>.
27. Hooper JE, Scott MP. Communicating with hedgehogs. *Nat Rev Mol Cell Biol*. 2005;6:306–17. <https://doi.org/10.1038/nrm1622>.
28. Sigafos AN, Paradise BD, Fernandez-Zapico ME. Hedgehog/GLI signaling pathway: transduction, regulation, and implications for disease. *Cancers (Basel)*. 2021;13:3410. <https://doi.org/10.3390/cancers1343410>.
29. de Van Wetering M, Castrop J, Korinek V, Clevers H. Extensive alternative splicing and dual promoter usage generate Tcf-1 protein isoforms with differential transcription control properties. *Mol Cell Biol*. 1996;16:745–52. <https://doi.org/10.1128/MCB.16.3.745>.
30. Kopelman NM, Lancet D, Yanai I. Alternative splicing and gene duplication are inversely correlated evolutionary mechanisms. *Nat Genet*. 2005;37:588–9. <https://doi.org/10.1038/ng1575>.
31. MacLean DW, Meedel TH, Hastings KEM. Tissue-specific alternative splicing of ascidian troponin I isoforms. *J Biol Chem*. 1997;272:32115–20. <https://doi.org/10.1074/jbc.272.51.32115>.
32. Holland LZ. Genomics, evolution and development of amphioxus and tunicates: the Goldilocks principle. *J Exp Zool B Mol Dev Evol*. 2015;324:342–52. <https://doi.org/10.1002/jez.b.22569>.
33. Huang X, Ren Q, Wang Y, Shimeld SM, Li G. Amphioxus Gli knockout disrupts the development of left-right asymmetry but has limited impact on neural patterning. *Mar Life Sci Technol*. 2023;5:492–9. <https://doi.org/10.1007/s42995-023-00195-w>.
34. Smith JJ, Kuraku S, Holt C, Sauka-Spengler T, Jiang N, Campbell MS, et al. Sequencing of the sea lamprey (*Petromyzon marinus*) genome provides insights into vertebrate evolution. *Nat Genet*. 2013;45:415–21. <https://doi.org/10.1038/ng.2568>.
35. Hotta K, Mitsuhashi K, Takahashi H, Inaba K, Oka K, Gojobori T, et al. A web-based interactive developmental table for the ascidian *Ciona intestinalis*, including 3D real-image embryo reconstructions: I. From fertilized egg to hatching larva. *Dev Dyn*. 2007;236:1790–805. <https://doi.org/10.1002/dvdy.21188>.
36. Tahara Y. Normal stages of development in the lamprey, *Lampetra reissneri* (Dybowski). *Zoolog Sci*. 1988;5:109–18. <https://doi.org/10.1038/s41392-023-01559-5>.

758

759

760

761

762

763

764

765

766

767

768

769

770

771

772

773

774

775

776

777

778

779

780

781

782

783

784

785

786

787

788

789

790

791

792

793

794

795

796

797

798

799

800

801

802

803

804

805

806

807

808

809

810

811

812

813

814

815

816

817

818

819

820

821

822

823

824

825

826

827

828

829 37. Zahn N, Levin M, Adams DS. The Zahn drawings: new illustrations of
830 *Xenopus* embryo and tadpole stages for studies of craniofacial develop-
831 ment. *Development*. 2017;144:2708–13. <https://doi.org/10.1242/dev.151308>.

832 38. Shen W, Le S, Li Y, Hu F. Seqkit: a cross-platform and ultrafast toolkit for
833 FASTA/Q file manipulation. *PLoS One*. 2016;11:e0163962. <https://doi.org/10.1371/journal.pone.0163962>.

834 39. Li H. New strategies to improve minimap2 alignment accuracy. *Bioinfor-
835 matics*. 2021;37:4572–4. <https://doi.org/10.1093/bioinformatics/btab705>.

836 40. Department of Zoology, Graduate School of Science, Kyoto University.
837 *Ciona intestinalis* KH genome assembly (GCA_000224145.2). NCBI Data-
838 sets. 2013. https://identifiers.org/ncbi/assembly:GCA_000224145.2.

839 41. Vertebrate Genomes Project. *Petromyzon marinus* (kPetMar1) genome
840 assembly. NCBI Datasets. 2020. https://identifiers.org/ncbi/assembly:GCA_010993605.1.

841 42. DOE Joint Genome Institute. *Xenopus tropicalis* (Xenopus_tropicalis_
842 v9.1) genome assembly (GCA_000004195.3). NCBI Datasets. 2016. https://identifiers.org/ncbi/assembly:GCA_000004195.3.

843 43. Wyman D, Mortazavi A. Transcriptclean: variant-aware correction of
844 indels, mismatches and splice junctions in long-read transcripts. *Bioinfor-
845 matics*. 2019;35:340–2. <https://doi.org/10.1093/bioinformatics/bty483>.

846 44. Kovaka S, Zimin V, Pertea GM, Razaghi R, Salzberg SL, Pertea M. Tran-
847 scriptome assembly from long-read RNA-seq alignments with StringTie2.
848 *Genome Biol*. 2019;20:278. <https://doi.org/10.1186/s13059-019-1910-1>.

849 45. Haas BJ. TransDecoder.

850 46. Manni M, Berkeley MR, Seppey M, Simão FA, Zdobnov EM. BUSCO
851 update: novel and streamlined workflows along with broader and deeper
852 phylogenetic coverage for scoring of eukaryotic, prokaryotic, and viral
853 genomes. *Mol Biol Evol*. 2021;38:4647–54. <https://doi.org/10.1093/molbev/msab199>.

854 47. Pertea G, Pertea M. GFF utilities: GffRead and GffCompare. F1000Res.
855 2020;9:304. <https://doi.org/10.12688/f1000research.23297.1>.

856 48. Cantalapiedra CP, Hernández-Plaza A, Letunic I, Bork P, Huerta-Cepas
857 J. eggNOG-mapper v2: functional annotation, orthology assignments,
858 and domain prediction at the metagenomic scale. *Mol Biol Evol*.
859 2021;38:5825–9. <https://doi.org/10.1093/molbev/msab293>.

860 49. Cao C, Lemaire LA, Wang W, Yoon PH, Choi YA, Parsons LR, et al. Compre-
861 hensive single-cell transcriptome lineages of a proto-vertebrate. *Nature*.
862 2019;571:349–54. <https://doi.org/10.1038/s41586-019-1385-y>.

863 50. Pang Y, Qin Y, Du Z, Liu Q, Zhang J, Han K, et al. Single-cell transcri-
864 ptope atlas of lamprey exploring Natterin- induced white adipose
865 tissue browning. *Nat Commun*. 2025;16:752. <https://doi.org/10.1038/s41467-025-56153-w>.

866 51. Liao Y, Ma L, Guo Q, E W, Fang X, Yang L, et al. Cell landscape of larval and
867 adult *Xenopus laevis* at single-cell resolution. *Nat Commun*. 2022;13:4306.
868 <https://doi.org/10.1038/s41467-022-31949-2>.

869 52. Marine Genomics Unit, Okinawa Institute of Science and Technology.
870 *Ciona intestinalis* (Cint(typeB-Roscoff)_1.0) genome assembly. NCBI
871 Datasets. 2021. https://identifiers.org/ncbi/assembly:GCA_018327825.1.

872 53. Marine Genomics Unit, Okinawa Institute of Science and Technology.
873 *Ciona intestinalis* (Cint(typeB-Plymouth)_1.0) genome assembly. NCBI
874 Datasets. 2021. https://identifiers.org/ncbi/assembly:GCA_018327805.1.

AQ8

Publisher's Note

Springer Nature remains neutral with regard to jurisdictional claims in published maps and institutional affiliations.

	Journal : BMCTwo 12915	Dispatch : 19-1-2026	Pages : 13
	Article No : 2522	<input type="checkbox"/> LE	<input type="checkbox"/> TYPESET
	MS Code :	<input checked="" type="checkbox"/> CP	<input checked="" type="checkbox"/> DISK

Journal:	12915
Article:	2522

Author Query Form

Please ensure you fill out your response to the queries raised below and return this form along with your corrections

Dear Author

During the process of typesetting your article, the following queries have arisen. Please check your typeset proof carefully against the queries listed below and mark the necessary changes either directly on the proof/online grid or in the 'Author's response' area provided below

Query	Details Required	Author's Response
AQ1	Please check if the affiliations are presented correctly. Otherwise, kindly amend if necessary.	
AQ2	Please check author names if captured correctly.	
AQ3	Please check if the section headings are assigned to appropriate levels. Otherwise, kindly amend if necessary.	
AQ4	Please check if table header, data, captions, citations and footnotes of all tables are presented correctly.	
AQ5	Please check if all figure caption and citations are captured and presented correctly.	
AQ6	NOTE: Figures 2 and 4 contains small text below the minimum required font size of 6pts inside the artwork, and there is no sufficient space available for the text to be enlarged. Please provide replacement figure file.	
AQ7	Please check if the additional file was captured and presented correctly.	
AQ8	Please provide complete bibliographic details for reference (45).	